IEEE Access
Multidisciplinary : Rapid Review : Open Access Journal

Received 29 July 2022, accepted 15 August 2022, date of publication 19 August 2022, date of current version 29 August 2022.

Digital Object Identifier 10.1109/ACCESS.2022.3200391

RESEARCH ARTICLE

N-White Balancing: White Balancing for Multiple Illuminants Including Non-Uniform Illumination

TERUAKI AKAZAWA[1], (Student Member, IEEE), YUMA KINOSHITA[2], (Member, IEEE), SAYAKA SHIOTA[1], (Member, IEEE), AND HITOSHI KIYA[1], (Life Fellow, IEEE)

[1]Department of Computer Science, Tokyo Metropolitan University, Tokyo 191-0065, Japan
[2]Department of Human and Information Science, Tokai University, Kanagawa 259-1292, Japan

Corresponding author: Hitoshi Kiya (kiya@tmu.ac.jp)

ABSTRACT In this paper, we propose a novel white balance adjustment for multi-illuminant scenes, called "N-white balancing," in which *N* source white points are mapped into a ground truth one. Most white balance adjustments focus on adjusting single-illuminant scenes. Several state-of-the-art methods for adjusting multi-illuminant scenes have been proposed, but they need to know the number of segments or the number of light sources in advance. Multi-color balance adjustments have been investigated to improve the performance of white balancing, but they also suffer from color distortion due to the rank deficiency problem. In contrast, the proposed method, N-white balancing, can correct multi-illuminant scenes even when we do not know the exact number of segments or light sources in a scene. In an experiment, the proposed method was demonstrated to outperform state-of-the-art methods under various illumination conditions such as single and multiple illuminants including non-uniform light sources.

INDEX TERMS Color constancy, color correction, image processing, white balance adjustment, multi-illuminant scene.

I. INTRODUCTION

Image segmentation and object recognition are required to decompose an image into meaningful regions. A typical approach to this problem assigns a single class to each pixel in an image. However, such hard segmentation is far from ideal when the distinction between meaningful regions is ambiguous, such as in the cases of objects with motion blur or color distortion caused by illumination or in the case of image enhancement [1], [2], [3], [4], [5]. Accordingly, we aim to reduce lighting effects in an image.

A change in illumination affects the pixel values of an image taken with an RGB digital camera because the values are determined by spectral information. In the human visual system, it is well known that illumination changes (i.e., lighting effects) are reduced, and this ability keeps the entire color perception of a scene constant. In contrast, since cameras do not essentially have this ability, white balancing is applied to images [6], [7], [8].

The associate editor coordinating the review of this manuscript and approving it for publication was Gustavo Callico.

Most traditional white balancing attempts to remove lighting effects on the assumption that a scene is captured under a single light source. Such white balancing for single illuminants (i.e., single-illuminant WB) requires two steps: estimating a source white point and mapping the estimated source white point into a ground truth white point without lighting effects, where "source white point" is a set of tristimulus values that represents the color of a white region when a light source strikes the white region, "white region" is a region that reflects all of the light, and "ground truth white point" is a source white point measured under an ideal light source such as the CIE standard illuminant D65 [9]. Accordingly, a source white point represents the color of illumination. In general, a source white point is calculated as a representative (e.g., the mean or median) value from the pixel values of the white region, and it is denoted by a set of tristimulus values such as (X, Y, Z) in the XYZ color space [10]. The phrase "source white point" is sometimes referred to as "illuminant." Many studies have focused on automatically estimating a source white point in an image [11], [12], [13], [14], [15], [16], [17], [18], [19], [20], [21], [22], [23], [24], [25], [26], [27],

[28], [29], [30], [31], [32], [33], [34]. Also, some methods automatically select the most appropriate algorithm for illuminant estimation depending on the content of individual images [35], [36], [37]. However, single-illuminant WB cannot reduce lighting effects under multiple illuminants. Mixed and non-uniform light sources are examples of multiple illuminants.

Multi-color balance adjustments [8], [38], [39] have been proposed to consider correcting various colors. In these methods, multiple colors are used for designing a matrix that maps multiple colors into ground truth colors. However, multi-color balancing may cause the rank deficiency problem to occur as a non-diagonal matrix is used, unlike white balancing [40].

To address this problem, state-of-the-art white balance adjustments for mixed light sources (i.e., multi-illuminant WB) have been proposed [25], [41], [42], [43], [44], [45]. By using a segment-wise estimation of a source white point, these methods can adjust lighting effects under single or mixed light sources. However, in some cases, the number of segments or the number of light sources needs to be known in advance [46]. Wrong assumptions result in color distortion in an image [45]. Moreover, these methods consider multiple illuminants as mixed light sources, so non-uniform illumination such as shading cannot effectively be adjusted. Barnard *et al.*'s method [47] considers non-uniform illumination. However, it assumes that the illuminant transition is smooth. Several approaches [26], [27], [48], [49] based on the human vision system (HVS) have been proposed, and some of them [48], [49] can be applied for adjusting multi-illuminant scenes. Also, methods based on machine learning [46], [50], [51], [52] have been studied. However, both HVS- and learning-based methods have problems such that any previously studied illuminant estimation algorithm cannot be used.

Accordingly, in this paper, we propose a novel white balancing called "N-white balancing" for adjusting images taken under single and multiple illuminants. N is the number of source white points, not the number of light sources. Under a general single-illuminant scene, N source white points have almost the same set of values. In contrast, under a multi-illuminant scene, source white points calculated from N different positions are generally different. The proposed method aims to simply adjust N source white points to corresponding ground truth ones. Hence, the method can reduce lighting effects under various illumination conditions even when N is a larger number than the number of light sources in a scene. Therefore, N-white balancing relieves us of needing to accurately select such parameters. Additionally, color distortion due to a rank deficient matrix is never caused in N-white balancing because a diagonal matrix is used.

In experiments, the proposed method was compared with single-illuminant WB, multi-color balancing, and multi-illuminant WB on the basis of the reproduction angular error [53].

TABLE 1. Differences among color balance adjustments.

Method	Light sources		Selection of source points	
	Single	Multiple	Achromatic	Chromatic
Single-illuminant WB	✓		✓	
Multi-color balancing	✓		✓	✓
Multi-illuminant WB (proposed method)	✓	✓	✓	

The rest of this paper is organized as follows. In Section II, we review related work. In Section III, we present our N-white balancing for single and multiple illuminants. In Section IV, we evaluate the effectiveness of the proposed method. In Section V, we conclude our research.

II. RELATED WORK

We summarize conventional methods for color constancy to clearly show problems with these methods. Conventional methods are categorized into three types: single-illuminant WB, multi-color balancing, and multi-illuminant WB. In Table 1, the differences among the color balance adjustments are summarized in terms of the number of light sources and the selection of source points. The proposed method is a type of multi-illuminant WB.

A. LIGHTING EFFECTS ON PIXEL VALUES

On the basis of the Lambertian model [54], the pixel values of an image taken with an RGB digital camera are determined by using three elements: spectra of illumination $E(\lambda)$, spectral reflectance of objects $S(\lambda)$, and camera spectral sensitivity R_C for color $C \in \{\mathrm{R}, \mathrm{G}, \mathrm{B}\}$, where λ spans the visible spectrum in the range of $[400, 720]$. A pixel value $\boldsymbol{P}_{\mathrm{RGB}} = (P_{\mathrm{R}}, P_{\mathrm{G}}, P_{\mathrm{B}})^\top$ in the camera RGB color space is given by

$$\boldsymbol{P}_{\mathrm{RGB}} = \int_{400}^{720} E(\lambda)S(\lambda)R_C(\lambda)\, d\lambda. \tag{1}$$

Eq. (1) means that a change in illumination $E(\lambda)$ affects the pixel values in an image. In the human visual system, the changes (i.e., lighting effects) are excluded, and the overall color perception is constant regardless of illumination differences, known as color constancy. To mimic this human ability as a computer vision task, white balancing (WB) is typically performed as a color adjustment technique.

B. WHITE BALANCING FOR SINGLE ILLUMINANT

Under a single light source, single-illuminant WB can reduce lighting effects on colors in an image. A two-step procedure is required to perform single-illuminant WB: 1) estimate a source white point, and 2) map the estimated source white point into a ground truth white point. Many studies on color constancy have focused on the first step (i.e., source white point estimation) [11], [12], [13], [14], [15], [16], [17], [18], [19], [20], [21], [22], [23], [24], [25], [26], [27], [28], [29], [30], [31], [32], [33], [34].

Methods for estimating a source white point are categorized into three types. The first type is methods that need the locations of white regions to calculate a source white point from white regions. Yang *et al.* proposed a method for estimating a source white point under the framework of the Grey-Pixels adjustment [25], and the method belongs to this first type. The second type is methods that determine a source white point from pixels satisfying a specific condition [11], [12], [15], [19], [24], [26], [27], [30], [55]. For example, the White-Patch algorithm assumes that the maximum pixel values in RGB channels represent a perfect reflectance of the light source [11]. These methods do not require that the locations of white regions be estimated, unlike the estimation method of the Grey-Pixels adjustment. The third type is methods that determine a source white point by using machine learning [13], [14], [16], [17], [20], [21], [22], [23], [28], [29], [32], [33], [34], [56], [57]. These approaches can also compute a source white point without estimating the locations of white regions. Therefore, the estimation methods of the second and third types enable us to estimate a source white point without white regions. Alternatively, they approximate the pixel values of white regions by using other pixel values in an image such as the maximum pixel value in the image. Performing both the first and the second steps is called "auto white balance adjustment" because white balance adjustment can be fully automated. In contrast, we may decide a source white point by manually pointing out a white region with remaining lighting effects under some conditions, which is called "manual white balance adjustment." Under these conditions, the error in illuminant estimation is ignored.

After obtaining illuminant information automatically or manually, the second step is performed by

$$\boldsymbol{P}_{\mathrm{WB}} = \mathbf{M}_{\mathrm{WB}}\boldsymbol{P}_{\mathrm{XYZ}}, \tag{2}$$

where $\boldsymbol{P}_{\mathrm{XYZ}} = (X_{\mathrm{P}}, Y_{\mathrm{P}}, Z_{\mathrm{P}})^\top$ is a pixel value of an image in the XYZ color space [10], and $\boldsymbol{P}_{\mathrm{WB}} = (X_{\mathrm{WB}}, Y_{\mathrm{WB}}, Z_{\mathrm{WB}})^\top$ is that of a white-balanced image [58]. $\mathbf{M}_{\mathrm{WB}}$ in (2) is given as

$$\mathbf{M}_{\mathrm{WB}} = \mathbf{M}_{\mathrm{A}}{}^{-1}\begin{pmatrix} \rho_{\mathrm{D}}/\rho_{\mathrm{S}} & 0 & 0 \\ 0 & \gamma_{\mathrm{D}}/\gamma_{\mathrm{S}} & 0 \\ 0 & 0 & \beta_{\mathrm{D}}/\beta_{\mathrm{S}} \end{pmatrix}\mathbf{M}_{\mathrm{A}}. \tag{3}$$

$\mathbf{M}_{\mathrm{A}}$ with a size of 3×3 is decided in accordance with an assumed chromatic adaptation transform [58]. $(\rho_{\mathrm{S}}, \gamma_{\mathrm{S}}, \beta_{\mathrm{S}})^\top$ and $(\rho_{\mathrm{D}}, \gamma_{\mathrm{D}}, \beta_{\mathrm{D}})^\top$ are calculated from an obtained source white point of a light source $(X_{\mathrm{S}}, Y_{\mathrm{S}}, Z_{\mathrm{S}})^\top$ in an input image and a ground truth white point $(X_{\mathrm{D}}, Y_{\mathrm{D}}, Z_{\mathrm{D}})^\top$ as

$$\begin{pmatrix} \rho_{\mathrm{S}} \\ \gamma_{\mathrm{S}} \\ \beta_{\mathrm{S}} \end{pmatrix} = \mathbf{M}_{\mathrm{A}}\begin{pmatrix} X_{\mathrm{S}} \\ Y_{\mathrm{S}} \\ Z_{\mathrm{S}} \end{pmatrix}, \begin{pmatrix} \rho_{\mathrm{D}} \\ \gamma_{\mathrm{D}} \\ \beta_{\mathrm{D}} \end{pmatrix} = \mathbf{M}_{\mathrm{A}}\begin{pmatrix} X_{\mathrm{D}} \\ Y_{\mathrm{D}} \\ Z_{\mathrm{D}} \end{pmatrix}. \tag{4}$$

Using the 3×3-identity matrix as $\mathbf{M}_{\mathrm{A}}$ indicates that white balancing is performed in the XYZ color space. Otherwise, von Kries's [59], [60] and Bradford's [61] chromatic adaptation transforms, which were also proposed for reducing lighting effects on all colors under the framework of white balancing [62], can be used. For example, under the use of Bradford's model, $\mathbf{M}_{\mathrm{A}}$ is given as

$$\mathbf{M}_{\mathrm{A}} = \begin{pmatrix} 0.8951 & 0.2664 & -0.1614 \\ -0.7502 & 1.7135 & 0.0367 \\ 0.0389 & -0.0685 & 1.0296 \end{pmatrix}. \tag{5}$$

Single-illuminant WB is a technique that maps a source white points under a single light source into a ground truth one as in (3). However, most techniques for single-illuminant WB do not consider the adjusting of spatially varying colors caused under mixed or non-uniform light sources. Accordingly, it suffers from such multiple illuminants in terms of color constancy. To address this problem, state-of-the-art white balance adjustments that assume multi-illuminant scenes have been proposed, as described in Section II-D.

C. MULTI-COLOR BALANCING

Multi-color balance adjustments [8], [38] have been proposed to consider adjusting multiple colors under single illuminants, while single-illuminant WB considers adjusting a single color (i.e., white). In these methods, multiple colors are used for designing a non-diagonal matrix that maps the multiple colors into ground truth colors. Hence, source white points under multiple illuminants may also be adjusted by using multi-color balancing. However, when we include multiple source white points as multiple colors, the non-diagonal matrix will be rank deficient. To avoid the rank deficiency problem, various chromatic colors in addition to white should be selected for the matrix design. However, automatic estimation of chromatic colors under illumination is difficult, unlike auto white balance adjustments.

D. WHITE BALANCING FOR MULTIPLE ILLUMINANT

Only a handful of methods [41], [42], [43], [44], [45], [46], [47], [50], [51], [52], [63], [64] have been proposed to correct multiple source white points under mixed light sources. Because multi-illuminant WB is a type of white balancing, illuminant estimation may be used; moreover, the rank deficiency problem is never caused. Early work in [42], [43], and [44] uses a segment-wise illuminant estimation that divides images into small segments. In these methods, estimated illuminants are clustered by using K-means clustering. However, it is difficult to exactly set the parameters of clustering in general scenes. Yang *et al.* proposed the Grey-Pixels adjustment for multiple illuminants [25] in addition to that for single ones. However, the Grey-Pixels adjustment used for single illuminants is different from that used for multiple illuminants, so this method is not applicable if it is difficult to distinguish single-illuminant scenes from multi-illuminant ones. Moreover, the method has to use the illuminant estimation algorithm proposed for the Grey-Pixels adjustment. Hussain *et al.*'s method [45] splits an input image into multiple segments using the K-means^{++} algorithm to improve the accuracy of the color adjustment. However, the authors reported that the number of segments significantly affected the accuracy [45]. Therefore, the conventional multi-illuminant WB requires the exact number of segments or light sources in advance [46]. Wrong assumptions may cause incorrect color correction in the methods. Additionally, non-uniform light sources (e.g., shading) are not considered in these methods. Zhang *et al.* and Gao *et al.* proposed multi-illuminant WB based on the HVS [48], [49]. These methods do not need to

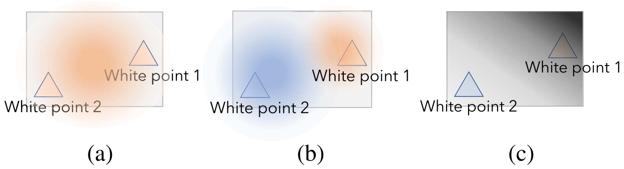

FIGURE 1. Overview of scenario ($N = 2$). (a) Single light source, (b) mixed light source, and (c) non-uniform light source.

set the number of clustering depending on the number of light sources. However, a more accurate mimic of realistic retinal mechanisms is required to improve the color correction performance, which has not been achieved yet [48]. Moreover, previously studied illuminant estimation algorithms cannot be used in these HVS-based methods since the HVS does not have the ability to estimate source white points directly.

A number of neural network-based methods have also been studied for multi-illuminant WB [46], [51], [52]. The performance of these methods is almost the same as that of multi-illuminant WB without a neural network. However, they suffer from two difficulties compared with multi-illuminant WB without a neural network: needing to collect a massive amount of images captured under multiple illuminants as training datasets and needing to implement a neural network in a camera system [46], [48].

Accordingly, this paper presents "N-white balancing" as a novel multi-illuminant WB. In the proposed method, N source white points are mapped into a ground truth one. Hence, the method does not need illuminant clustering. Also, N source white points can be manually decided or automatically estimated with every type of illuminant estimation algorithm. The proposed method focuses on simply correcting N source white points, for which we do not need to choose the correct number of light sources or segments as N, but some other adjustments for multi-illuminant scenes need it. Moreover, the method does not include complex tasks such as an accurate mimic of realistic retinal mechanisms, compared with methods based on the HVS [48], [49]. Therefore, the method can adjust images with no distinction between single- and multi-illuminant scenes, unlike the Grey-Pixels adjustment.

III. PROPOSED METHOD

Here, our novel multi-illuminant WB method, "N-white balancing," is proposed.

A. OVERVIEW OF PROPOSED METHOD

Even when the color of an object is white, it may be different from the white under a light source. If we select several source white points in a general single-illuminant scene, they may have almost the same set of values in general (see Fig. 1 (a)). In contrast, in a multi-illuminant scene such as one with mixed and non-uniform light sources, the values of source white points calculated from white regions in spatially different positions are generally different. (see Figs. 1 (b)–(c)). The proposed method individually adjusts N source white points to a ground truth one. Hence, the method can stably reduce lighting effects even when N is a larger number than the number of light sources in a scene. Colors among N source white points are also corrected by using N weights.

B. N-WHITE BALANCING

The proposed method is carried out by using N source white points, and they are combined with weights. In the method, a pixel value $\boldsymbol{P}_{\mathrm{XYZ}} = (X_{\mathrm{P}}, Y_{\mathrm{P}}, Z_{\mathrm{P}})^\top$ is adjusted to $\boldsymbol{P}'_{\mathrm{WB}} = (X'_{\mathrm{WB}}, Y'_{\mathrm{WB}}, Z'_{\mathrm{WB}})^\top$ as

$$\boldsymbol{P}'_{\mathrm{WB}} = \mathbf{M}'_{\mathrm{WB}} \boldsymbol{P}_{\mathrm{XYZ}}. \tag{6}$$

In general, ground truth white points have the same value as $\boldsymbol{G}_1 = \boldsymbol{G}_2 = \cdots = \boldsymbol{G}_N$, so $\mathbf{M}'_{\mathrm{WB}}$ in (6) is designed in a similar way to white balancing:

$$\mathbf{M}'_{\mathrm{WB}} = \mathbf{M}_{\mathrm{A}}{}^{-1} \begin{pmatrix} \rho'_{\mathrm{D}}/\rho'_{\mathrm{S}} & 0 & 0 \\ 0 & \gamma'_{\mathrm{D}}/\gamma'_{\mathrm{S}} & 0 \\ 0 & 0 & \beta'_{\mathrm{D}}/\beta'_{\mathrm{S}} \end{pmatrix} \mathbf{M}_{\mathrm{A}}, \tag{7}$$

where

$$\begin{pmatrix} \rho'_{\mathrm{S}} \\ \gamma'_{\mathrm{S}} \\ \beta'_{\mathrm{S}} \end{pmatrix} = \mathbf{M}_{\mathrm{A}} \left(k_1 \boldsymbol{S}_1 + k_2 \boldsymbol{S}_2 + \cdots + k_n \boldsymbol{S}_N \right), \quad \text{and}$$
$$\begin{pmatrix} \rho'_{\mathrm{D}} \\ \gamma'_{\mathrm{D}} \\ \beta'_{\mathrm{D}} \end{pmatrix} = \mathbf{M}_{\mathrm{A}} \left(k_1 \boldsymbol{G}_1 + k_2 \boldsymbol{G}_2 + \cdots + k_n \boldsymbol{G}_N \right). \tag{8}$$

$\boldsymbol{S}_m = (X_{\mathrm{S}m}, Y_{\mathrm{S}m}, Z_{\mathrm{S}m})^\top$ is the mth source white point ($m \in \{1, 2, \cdots, N\}$) in the XYZ color space, and k_m is a weight of $\boldsymbol{S}_m$ and $\boldsymbol{G}_m$. In a manner like the conventional white balancing, $\mathbf{M}_{\mathrm{A}}$ is used for accurately adjusting colors other than achromatic colors. The 3×3-identity matrix is used as $\mathbf{M}_{\mathrm{A}}$ when the proposed method is performed in the XYZ color space. von Kries's model or Bradford's one may also be used as $\mathbf{M}_{\mathrm{A}}$. As mentioned in Section II-B, the effectiveness of $\mathbf{M}_{\mathrm{A}}$ has been confirmed for single-illuminant scenes. In this paper, we verify the effectiveness of $\mathbf{M}_{\mathrm{A}}$ for multi-illuminant scenes in Section IV.

When the spatial pixel coordinate of $\boldsymbol{P}_{\mathrm{XYZ}}$ is closer to that of source white point $\boldsymbol{S}_m$ than the other ones, $\boldsymbol{S}_m$ should more contribute to adjusting $\boldsymbol{P}_{\mathrm{XYZ}}$ than the rest of the source white points. Hence, to measure the distance between the coordinates of $\boldsymbol{P}_{\mathrm{XYZ}}$ and $\boldsymbol{S}_m$, the Euclidean distance is calculated as

$$d_m = \sqrt{(x_{\mathrm{S}m} - x_{\mathrm{P}})^2 + (y_{\mathrm{S}m} - y_{\mathrm{P}})^2}, \tag{9}$$

where $(x_{\mathrm{S}m}, y_{\mathrm{S}m})$ is a pair of coordinates of $\boldsymbol{S}_m$, and $(x_{\mathrm{P}}, y_{\mathrm{P}})$ is that of $\boldsymbol{P}_{\mathrm{XYZ}}$. A smaller d_m means that $(x_{\mathrm{P}}, y_{\mathrm{P}})$ is closer to $(x_{\mathrm{S}m}, y_{\mathrm{S}m})$. Because k_m in (8) should be larger under a smaller d_m, the inverse proportion to d_m is calculated as

$$d'_m = \frac{1}{d_m}. \tag{10}$$

To reduce the total value of weights to 1 in (8), k_m is given as

$$k_m = \frac{d'_m}{d'_1 + d'_2 + \cdots + d'_N}. \tag{11}$$

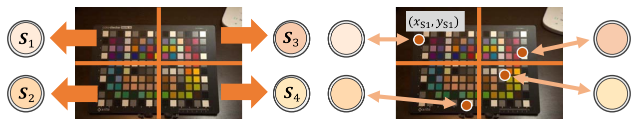

(a) (b)

FIGURE 2. Procedures with automatically estimated source white points ($N = 4$). (a) Applying block-wise illuminant estimation, and (b) deciding coordinates of source white points.

Note that, in (11), k_m will be infinite if the pixel coordinate of input pixel $\boldsymbol{P}_{\mathrm{XYZ}}$ is equal to that of $\boldsymbol{S}_m$ (i.e., $d_m = 0$). In this case, let k_m be a value of 1, and let the other weights be a value of zero. In the proposed method, the use of the Euclidean distance derives from the Grey-Pixels adjustment for multi-illumination [25]. However, the calculations are different from the Grey-Pixels adjustment as in (10)–(11), and there is no parameter such as the weighting sensitivity that Grey-Pixels has.

C. PROCEDURE OF N-WHITE BALANCING

To perform the proposed method, three sets of data are prepared: a ground truth white point $\boldsymbol{G} = (X_{\mathrm{G}}, Y_{\mathrm{G}}, Z_{\mathrm{G}})^\top$, N source white points $\boldsymbol{S}_m = (X_{\mathrm{S}m}, Y_{\mathrm{S}m}, Z_{\mathrm{S}m})^\top$ $(m \in \{1, 2, \cdots, N\})$, and the pixel coordinates $(x_{\mathrm{S}m}, y_{\mathrm{S}m})$ corresponding to the N source white points. The procedure of the proposed method is carried out as below.

1) Decide a ground truth white points as $\boldsymbol{G}$.
2) Prepare white regions in various locations of a camera frame to compute $\boldsymbol{S}_m$.
3) Obtain the pixel coordinates $(x_{\mathrm{S}m}, y_{\mathrm{S}m})$ of $\boldsymbol{S}_m$.
4) Apply N-white balancing, following Section III-B.

N-white balancing is a kind of multi-illuminant WB, so illuminant estimation algorithms can be used instead of preparing white regions in step 2). For example, to automatically estimate N source white points, block segmentation is applied to an image, and a block-wise illuminant estimation algorithm can be used (see Fig. 2 (a)). In this paper, the cosine similarity between $\boldsymbol{S}_m$ and the pixels of each block is calculated, and the coordinates of the closest pixel to $\boldsymbol{S}_m$ are decided as $(x_{\mathrm{S}m}, y_{\mathrm{S}m})$ (see Fig. 2 (b)).

In the proposed method, the locations of N source white points are used, which are decided from estimated source white points and the pixels of each block. The method does not need the locations of white regions, unlike the Grey-Pixels adjustment [25]. As discussed in Section II, this is because some methods that estimate a source white point without white regions have been proposed, and these methods can be applied to the illuminant estimation part of the proposed method.

D. PROPERTIES OF N-WHITE BALANCING

The properties that the proposed N-white balancing has are summarized here.

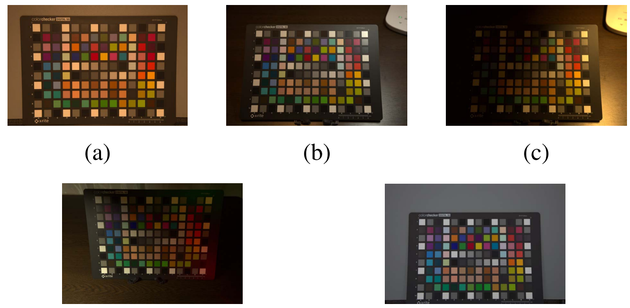

(a) (b) (c)
(d) (e)

FIGURE 3. Images taken under different lighting conditions. (a) Single artificial light source, (b) two artificial (i.e., mixed) light sources, (c) non-uniform light source, (d) three artificial light sources with non-uniformity (i.e., complex light source), and (e) ground truth image.

(a) The rank deficiency problem is never caused since a diagonal matrix is used as in (7), unlike multi-color balancing.
(b) N does not need to correspond to the exact number of light sources or segments.
(c) Source white points may be selected manually in addition to automatically estimating them.
(d) Any previously studied algorithm can be used for the illuminant estimation part of N-white balancing.

In N-white balancing, we apply block segmentation to decide N source white points as described in Section III-C, so the proposed method is effective in adjusting multi-illuminant scenes including non-uniform illumination. In addition, when using a fixed-point camera, source white points may manually be decided, so that the performance is improved and the process is simplified.

IV. EXPERIMENTS

We conducted experiments to confirm the effectiveness of the proposed method.

A. EXPERIMENTAL SETUP

In the first experiment, we used five images taken under various illumination conditions such as single, mixed, and non-uniform light sources, where each image included a color rendition chart (see Fig. 3). In this experiment, source white points were manually decided from the white regions in the color rendition charts or automatically estimated by using an illuminant estimation algorithm. We also confirmed that the performance of N-white balancing was maintained regardless of N. Note that the proposed method and single-illuminant WB were combined with Bradford's model [61]. The performance of each method was evaluated by using the reproduction angular error [53] between a mean-pixel vector of an adjusted object's region $\boldsymbol{P}$ and that of the corresponding ground truth one $\boldsymbol{Q}$. The reproduction error between $\boldsymbol{P}$ and $\boldsymbol{Q}$ is given by

$$E_{\mathrm{rep}} = \frac{180}{\pi} \cos^{-1}\left(\frac{\boldsymbol{P} \cdot \boldsymbol{Q}}{\|\boldsymbol{P}\|\|\boldsymbol{Q}\|}\right) \quad [\mathrm{deg}]. \tag{12}$$

In the second experiment, we used the two-illuminant dataset [43], which consists of 58 laboratory images taken under close-to-ideal conditions and 20 real-world images. Similarly to the previous experiment with color rendition charts, we demonstrated that the proposed method was also effective in adjusting images taken in general scenes. In this experiment, our error metric per image was the mean pixel-wise angular error between estimated illuminant $\boldsymbol{i}$ and the corresponding ground truth one $\boldsymbol{j}$, given as

$$E_{\mathrm{ang}} = \frac{180}{\pi n_{\mathrm{p}}} \sum_{i=1}^{n_{\mathrm{p}}} \cos^{-1}((\boldsymbol{i}_i)^\top \cdot \boldsymbol{j}_i) \ \ [\mathrm{deg}], \tag{13}$$

where n_{p} is the number of pixels in an image.

In the third experiment, we used two state-of-the-art datasets: the LSMI dataset [65] and Afifi *et al.*'s mixed-illuminant test set [46]. The LSMI dataset consists of natural scenes in the real world, and it has three subsets named "galaxy," "nikon," and "sony." In this experiment, we used 1,124 two-illuminant scenes in the galaxy subset, and the performance of each method was evaluated by using the mean pixel-wise angular error as in (13). Afifi *et al.*'s mixed-illuminant test set includes 150 synthetic images rendered by 3Ds Max. In this dataset, the reproduction angular error as in (12) was used to evaluate each method.

B. EXPERIMENTAL RESULTS WITH MANUALLY DECIDED SOURCE WHITE POINTS

The effectiveness of N-white balancing was confirmed under the use of manually decided source white points.

1) EVALUATION OF SINGLE AND MULTIPLE ILLUMINANTS

In this experiment, we first confirmed that the proposed method is effective for correcting both single- and multiple-illuminant scenes. By using source white points decided from the white regions in a color rendition chart, the proposed method was compared with single-illuminant WB and multi-color balancing [8].

Figure 4 shows the adjusted images for Figs. 3 (a)–(d). The heat map below each image indicates the reproduction angular error for every color patch, where $\boldsymbol{P}$ in (12) is the representative pixel value of one of the color patches in an adjusted image for Figs. 3 (a)–(d), and $\boldsymbol{Q}$ is that for the ground truth image (see Fig. 3 (e)). The mean value of the pixel values in a color region (i.e., color patch) was used as a representative value. Also, the mean value (Mean) and the standard variation (Std) of all color patches are shown next to each heat map. Note that patches whose color is pure black were excluded from the calculation of Mean and Std because the metric cannot precisely measure errors against low surface reflectances. Source white points were decided from white regions represented as the green rectangle in the figures.

As shown in Fig. 4, the proposed method reduced both single- and multi-illuminant effects, and it had the lowest mean error in all situations. In contrast, the multi-illuminant scenes were not adjusted by single-illuminant WB, although the single-illuminant scene was corrected as well as the proposed method. Also, multi-color balancing caused the rank deficiency problem to occur, and the chromatic colors were distorted.

2) INFLUENCE OF SELECTING N

Figure 5 shows the relationship between mean errors and N (i.e., the number of source white points). In Figs. 3 (a) and (b), the scene was taken under a single light source and two different light sources, respectively. As shown in Fig. 5 (b), when N was below the number of light sources in the scene, N-white balancing could not correctly adjust the images. However, when N was larger than the number of light sources, the performance of N-white balancing was maintained. Therefore, N does not need to correspond to the exact number of light sources.

C. EXPERIMENTAL RESULTS WITH AUTOMATICALLY ESTIMATED SOURCE WHITE POINTS

In this section, the effectiveness of N-white balancing is demonstrated under the use of automatically estimated source white points.

1) EVALUATION OF SINGLE AND MULTIPLE ILLUMINANTS

First, the proposed method with manually decided source white points was compared with automatically estimated ones. In this experiment, the White-Patch algorithm [11] was used for estimating source white points. Also, a block size of 3×3 was decided for the proposed method as the performance of the method is maintained when N is larger than the number of light sources in a scene (see Section III-C). Figure 6 shows a comparison between manual white balancing and automatic white balancing. The performance of color correction did not significantly differ between using manually decided source white points and using automatically estimated ones in these images. Also, the use of source white points manually selected from white regions (i.e., manual white balance adjustments) slightly improved the performance of the color adjustments. Therefore, the effectiveness of property (III-D) in Section III-D was confirmed, while the conventional multi-illuminant WB can only be used for auto white balance adjustments.

In following experiments, we confirmed that the proposed method is effective as an automatic white balance adjustment in adjusting images under single and multiple illuminants. In this experiment, the proposed method, single-illuminant WB, and multi-illuminant WB [25], [42], [45], [46], [48] were tested by using the White-Patch algorithm [11], which is a typical illuminant estimation method. The number of illuminants was set to two in Gijsenij *et al.*'s and Yang *et al.*'s method [25], [42], and the number of segments was set to four in Hussain *et al.*'s method [45], and these settings were recommended by the respective authors.

Table 2 shows the Mean and Std of the reproduction angular errors for the white balance adjustments.

FIGURE 4. Adjusted images for Figs. 3 (a)–(d). (a) No adjustment, (b) single-illuminant WB, (c) multi-color balancing, (d) proposed method, and (e) color bar of heat maps. In (a)–(d), four images correspond to Figs. 3 (a)–(d), respectively.

The proposed method outperformed the conventional single- and multi-illuminant WB in terms of mean errors. In addition, the effectiveness of single-illuminant WB was confirmed for the single-illuminant scene, which showed the same trend as that seen in Section IV-B1. The multi-illuminant WB without a neural network [25], [42], [45], [48] had unstable performance depending on the illumination conditions, while the proposed method stably adjusted images under such conditions. The multi-illuminant WB based on a neural network by Afifi *et al.* [46] suppressed single- and multi-illuminant effects; however, the Mean and Std of the angular errors were higher than those for the proposed method. Therefore, the effectiveness of the proposed method for single and multiple illuminants including non-uniform light sources was confirmed.

2) INFLUENCE OF USING SAME N FOR VARIOUS ILLUMINATION CONDITIONS

As mentioned, in the proposed method, N does not need to correspond to the exact number of light sources or the exact number of scene segments. In this section, the proposed method was compared with multi-illuminant WB [42], [45] without a neural network by changing parameters.

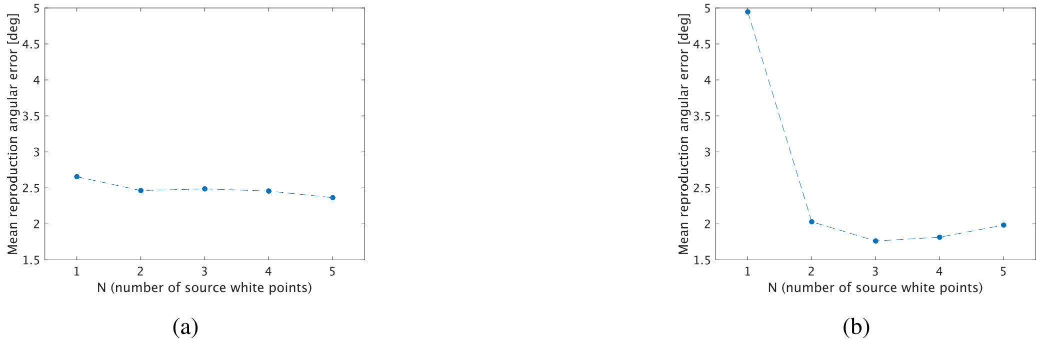

FIGURE 5. Mean reproduction angular error in N-white balancing. (a) Mean errors of adjusted images for Figs. 3 (a) and (b) those for Fig. 3(b).

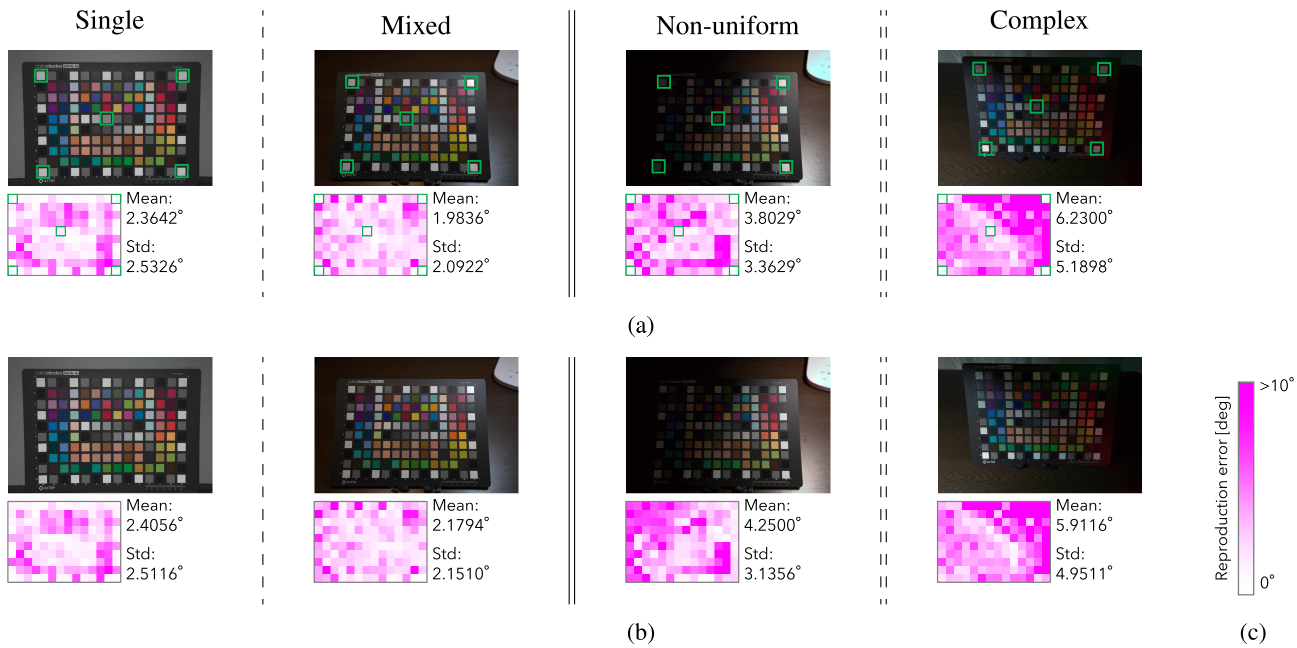

FIGURE 6. Images from Figs. 3 (a)–(d) adjusted by using manually decided source white points or automatically estimated ones. (a) Proposed method with manually decided source white points, (b) proposed method with White-Patch algorithm, and (c) color bar of heat maps.

Figure 7 shows adjusted images for Fig. 3 (a). Two different parameters were tested in Gijsenij *et al.*'s method [42] as shown in Figs. 7 (b) and (c); the number of illuminants was modified from two to one because only one light source illuminated the scene. Figure 8 shows adjusted images for Fig. 3 (b). Two different parameters were tested in Hussain *et al.*'s method [45] as shown in Figs. 8 (b) and (c); the number of segments was reduced from four to two because there were two light sources. Comparing Figs. 7 (b) and 8 with Figs. 7 (c) and 8 (c), respectively, the conventional multi-illuminant WB [42], [45] may require the exact number of light sources or segments, and accurately adjusting the parameters significantly contributed to improving the performance. In contrast, the proposed method could be carried out without changing N.

3) EVALUATION WITH TWO-ILLUMINANT DATASET

In Sections IV-B, IV-C1, and IV-C2, we prepared five images taken under various illumination conditions. However, the images were far different from those taken under general scenes. To test the proposed method under usual photographing conditions, we used the two-illuminant dataset [43] and compared the proposed method with single-illuminant WB [58] and multi-illuminant WB [25], [42], [43], [45], [48], [49], [51]. Also, the proposed method, single-illuminant WB [58], and methods for multi-illuminant scenes [42], [43] were carried out with nine illuminant estimation algorithms: White-Patch (WP) [11], Grey-World (GW) [12], Shades-of-Gray (SoG) [15], 1st-order Grey-Edge (GE1) [19], 2nd-order Grey-Edge (GE2) [19], PCA [24], Grey-Pixels for single-illuminant estimation [GP(std)] [25], Mean-Shifted Grey-Pixels (MSGP) [31], and Quasi-Unsupervised Color Constancy (QUCC) [32]. Table 3 shows the angular errors for images in the two-illuminant dataset. From the table, the proposed method outperformed single-illuminant WB, and it had almost the same performance as multi-illuminant WB. In particular, the proposed method had a lower angular error than Gijsenij *et al.*'s method [42], MIRF [43], Grey-Pixels

TABLE 2. Mean and standard variation of angular errors (deg) of adjusted images for Figs. 3 (a)–(d), where bold denotes minimum angular error in each column. Conventional methods and proposed method were applied by using automatically estimated source white points.

Color balance adjustment	Single-illuminant scenes		Multi-illuminant scenes					
	Fig. 3 (a)		Fig. 3 (b)		Fig. 3 (c)		Fig. 3 (d)	
	Mean	Std	Mean	Std	Mean	Std	Mean	Std
No adjustment	19.0545	6.5402	9.0262	3.7556	22.7800	8.8998	16.1690	8.1675
Single-illuminant WB	2.4757	2.5359	3.2525	2.4854	6.8270	**3.0796**	10.5257	8.5194
Gijsenij *et al.* [42]	54.5838	28.2670	4.4710	**2.0616**	93.9538	30.2547	66.4607	34.8223
GP (std) (M=2) [25]	2.6057	2.1181	2.6758	2.4597	5.1566	3.6573	9.2810	8.5935
Zhang *et al.* [48]	10.9226	8.1916	15.9430	6.7110	21.8980	8.2547	23.3541	12.2058
Hussain *et al.* [45]	3.0764	**2.1227**	9.1743	4.8078	7.7100	4.2210	9.2952	8.5373
Afifi *et al.* [46]	4.9438	3.5930	4.1081	3.5839	6.8798	5.1191	7.8641	7.0392
Proposed method	**2.4056**	2.5116	**2.1794**	2.1510	**4.2500**	3.1356	**5.9116**	**4.9511**

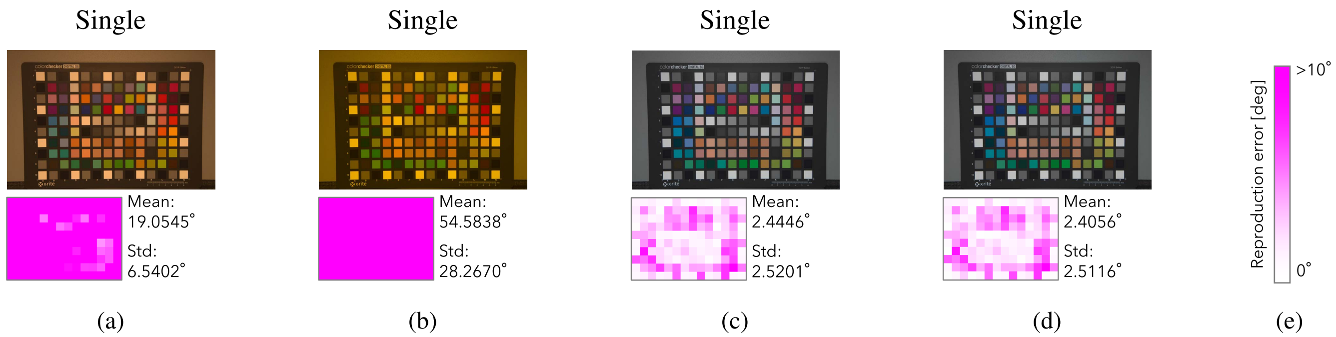

FIGURE 7. Images for Fig. 3 (a) adjusted using Gijsenij *et al.*'s method with two different parameters. (a) No adjustment, (b) Gijsenij *et al.*'s method where number of illuminants is two, (c) Gijsenij *et al.*'s method where number of illuminants is one, (d) proposed method, and (e) color bar of heat maps.

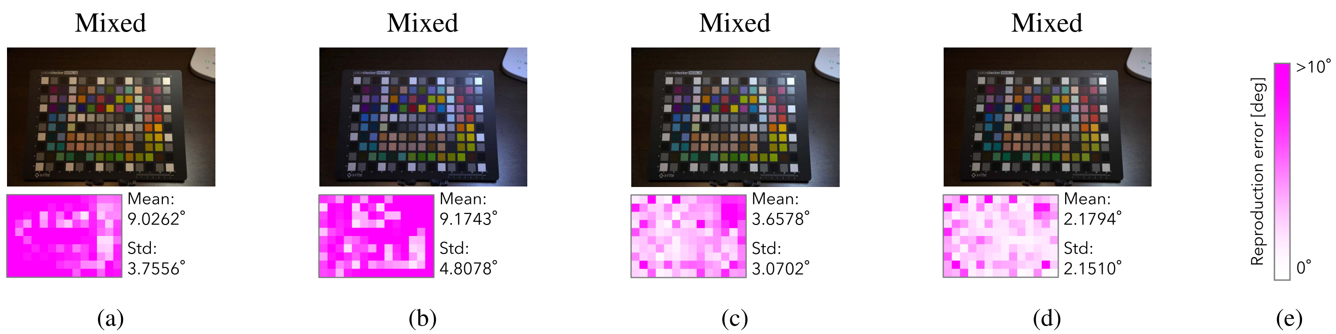

FIGURE 8. Images for Fig. 3 (b) adjusted using Hussain *et al.*'s method with two different parameters. (a) No adjustment, (b) Hussain *et al.*'s method where number of segments is four, (c) Hussain *et al.*'s method where number of segments is two, (d) proposed method, and (e) color bar of heat maps.

for multiple illuminants [25], Zhang *et al.*'s method [48], and BU-MCC [49]. For the laboratory set, Hussain *et al.*'s method [45] had a slightly lower error than the proposed method because the optimal number of segments (= 4) was prepared for this experiment. However, if a different number of segments were chosen, the performance of Hussain *et al.*'s method would decrease [45]. In contrast, the proposed method can maintain a high accuracy under various N values as described in Figs. 7 and 8. For the real set, TD-MCC [49] and Bianco *et al.*'s method with a neural network [51] also obtained competitive performance compared to the proposed method because a large amount of carefully prepared training data could be used.

In addition to the angular error, adjusted images should be subjectively compared. Figure 9 shows adjusted images for four sample images from the dataset. When we subjectively compared the proposed method with the conventional multi-illuminant WB [42], [45], the proposed method showed a more improved color constancy than the conventional methods despite some of the higher angular errors. Therefore, we confirmed that the proposed method is also effective for images where general scenes are captured.

4) EVALUATION WITH STATE-OF-THE-ART DATASETS

In this experiment, we evaluated the performance of the proposed method by using the LSMI dataset [65] and Afifi *et al.*'s mixed-illuminant test set [46]. In this experiment, the method was compared with single-illuminant WB [58], multi-illuminant WB [25], [42], [45]. Also, Zhang *et al.*'s method was compared with the proposed method on Afifi *et al.*'s mixed-illuminant test set.

TABLE 3. Mean and median angular errors (deg) for conventional methods and proposed method on two-illuminant dataset, where bold denotes minimum angular error in each column.

Color balance adjustment		Lab set		Real set	
		Mean	Med	Mean	Med
No adjustment		10.6	10.5	8.8	8.9
Single-illuminant WB	GW	3.2	2.9	5.2	4.2
	WP	7.8	7.6	6.8	5.6
	SoG	4.9	4.6	6.2	3.7
	GE1	3.1	2.8	5.3	3.9
	GE2	3.2	2.9	6.0	4.7
	PCA	4.1	3.7	7.6	3.4
	GP(std)	5.5	5.5	6.1	6.4
	MSGP	5.8	5.7	4.9	3.9
	QUCC	3.7	3.1	5.2	3.5
Gijsenij *et al.* [42]	GW	6.4	5.9	4.4	4.3
	WP	5.1	4.2	4.2	3.8
	GE1	4.8	4.2	9.1	9.2
	GE2	5.9	5.7	12.4	12.4
MIRF [43]	GW	3.1	2.8	3.7	3.4
	WP	3.0	2.8	4.1	3.3
	GE1	2.7	2.6	4.0	3.4
	GE2	2.6	2.6	4.9	4.5
GP(std)($M = 2$) [25]	–	3.1	2.5	5.7	3.3
Zhang *et al.* [48]	–	3.2	2.7	5.2	4.3
BU-MCC [49]	–	3.7	3.4	5.0	4.0
TD-MCC [49]	–	2.8	2.5	3.8	**2.9**
Bianco *et al.* [51]	–	2.3	2.2	**3.3**	3.1
Hussain *et al.* [45]	WP	**1.6**	**1.5**	3.8	3.9
Proposed method	GW	3.7	3.1	4.6	4.5
	WP	2.6	2.2	4.1	3.4
	SoG	2.8	2.3	4.2	3.8
	GE1	2.5	2.2	4.7	3.6
	GE2	2.6	2.5	4.7	4.0
	PCA	2.5	2.1	5.1	4.3
	GP(std)	2.3	2.1	3.7	3.0
	MSGP	2.3	2.2	3.7	3.3
	QUCC	3.1	2.7	4.0	3.4

TABLE 4. Mean and median angular errors (deg) for conventional methods and proposed method on the LSMI dataset, where bold denotes minimum angular error in each column.

Color balance adjustment		Mean	Med
No adjustment		17.4	17.0
Single-illuminant WB	GW	11.3	8.8
	WP	12.8	14.3
	GE1	12.1	10.8
	PCA	10.9	10.7
	GP(std)	16.8	17.0
Gijsenij *et al.* [42]	WP	18.0	17.4
GP(std)($M = 2$) [25]	–	17.1	17.0
Hussain *et al.* [45]	WP	17.7	16.9
Proposed method	GW	13.9	13.1
	WP	9.6	8.8
	GE1	12.1	10.8
	PCA	**8.3**	**7.4**
	GP(std)	12.4	11.2

The proposed method and single-illuminant WB [58] were carried out with five illuminant estimation algorithms: White-Patch (WP) [11], Grey-World (GW) [12], 1st-order Grey-Edge (GE1) [19], PCA [24], and Grey-Pixels for single-illuminant estimation [GP(std)] [25]. Tables 4 and 5 show experimental results on the LSMI dataset and Afifi *et al.*'s mixed-illuminant test set, respectively. From the tables, the proposed method outperformed the conventional methods. Therefore, the effectiveness of the proposed method was confirmed under the use of the state-of-the-art datasets.

FIGURE 9. Adjusted images from two-illuminant dataset. (a) No adjustment, (b) Gijsenij *et al.*, (c) Hussain *et al.*, (d) proposed method, and (e) ground truth. Note that images were converted to sRGB color space. Captions of each image denote mean angular error in image.

TABLE 5. Mean and median reproduction angular errors (deg) for conventional methods and proposed method on Afifi *et al.*'s mixed-illuminant test set, where bold denotes minimum angular error in each column.

Color balance adjustment		Mean	Med
No adjustment		19.7	17.2
Single-illuminant WB	GW	11.9	11.7
	WP	15.1	13.9
	GE1	12.6	12.0
	PCA	14.9	13.8
	GP(std)	16.2	15.0
Gijsenij *et al.* [42]	WP	23.2	19.9
GP(std)($M = 2$) [25]	–	11.9	11.5
Zhang *et al.* [48]	–	15.0	14.1
Hussain *et al.* [45]	WP	14.3	13.5
Proposed method	GW	10.8	10.5
	WP	11.4	10.5
	GE1	12.6	12.0
	PCA	11.1	10.3
	GP(std)	**10.3**	**9.9**

V. CONCLUSION

In this paper, we proposed a novel white balance adjustment for single and multiple illuminants including non-uniform light sources. The proposed method, called "N-white balancing," maps N source white points into a ground truth one. While traditional single-illuminant white balancing considers adjusting a source white point under a light source, N-white balancing can reduce lighting effects under multiple illuminants in addition to single ones. Only a handful of methods have been proposed to correct multi-illuminant scenes; however, in several methods, the exact number of light sources or the exact number of scene segments need to be known in advance. In contrast, in the proposed method, N does not need to correspond to the exact number of light sources or segments. Additionally, color distortion is never caused in the proposed method because a diagonal matrix is used, unlike multi-color balancing. In experiments, the proposed method and the conventional methods were evaluated by using various illumination conditions. The results show that N-white balancing outperformed the conventional methods. By improving the accuracy of color correction under various illumination conditions, the proposed method is expected to contribute to increasing the number of color-based applications in the future. In future work, we would like to demonstrate object recognition and other applications by purposely using the color information adjusted by the proposed method.

REFERENCES

[1] M. Afifi and M. Brown, "What else can fool deep learning? Addressing color constancy errors on deep neural network performance," in *Proc. IEEE/CVF Int. Conf. Comput. Vis. (ICCV)*, Oct. 2019, pp. 243–252.

[2] N. Akimoto, H. Zhu, Y. Jin, and Y. Aoki, "Fast soft color segmentation," in *Proc. IEEE/CVF Conf. Comput. Vis. Pattern Recognit. (CVPR)*, Jun. 2020, pp. 8274–8283.

[3] Y. Kinoshita and H. Kiya, "Hue-correction scheme based on constant-hue plane for deep-learning-based color-image enhancement," *IEEE Access*, vol. 8, pp. 9540–9550, 2020.

[4] Y. Kinoshita and H. Kiya, "Hue-correction scheme considering CIEDE2000 for color-image enhancement including deep-learning-based algorithms," *APSIPA Trans. Signal Inf. Process.*, vol. 9, no. 1, pp. 1–10, Sep. 2020.

[5] Y. Kinoshita and H. Kiya, "Scene segmentation-based luminance adjustment for multi-exposure image fusion," *IEEE Trans. Image Process.*, vol. 28, no. 8, pp. 4101–4116, Aug. 2019.

[6] D. H. Foster, "Color constancy," *Vis. Res.*, vol. 51, no. 7, pp. 674–700, Apr. 2011.

[7] A. Gijsenij, T. Gevers, and J. van de Weijer, "Computational color constancy: Survey and experiments," *IEEE Trans. Image Process.*, vol. 20, no. 9, pp. 2475–2489, Feb. 2011.

[8] D. Cheng, B. Price, S. Cohen, and M. S. Brown, "Beyond white: Ground truth colors for color constancy correction," in *Proc. IEEE Int. Conf. Comput. Vis. (ICCV)*, Dec. 2015, pp. 298–306.

[9] *Colorimetry—Part 2: CIE Standard Illuminants*, Standard ISO 11664–2:2007, ISO/CIE, 2007.

[10] *Commission Internationale de l'Eclairage Proceedings*, CIE, Cambridge Univ. Press, Cambridge, U.K., 1932.

[11] E. H. Land and J. J. McCann, "Lightness and Retinex theory," *J. Opt. Soc. Amer.*, vol. 61, no. 1, pp. 1–11, Jan. 1971.

[12] G. Buchsbaum, "A spatial processor model for object colour perception," *J. Franklin Inst.*, vol. 310, no. 1, pp. 1–26, Jul. 1980.

[13] D. A. Forsyth, "A novel algorithm for color constancy," *Int. J. Comput. Vis.*, vol. 5, no. 1, pp. 5–35, Aug. 1990.

[14] G. D. Finlayson, S. D. Hordley, and P. M. Hubel, "Color by correlation: A simple, unifying framework for color constancy," *IEEE Trans. Pattern Anal. Mach. Intell.*, vol. 23, no. 11, pp. 1209–1221, Nov. 2001.

[15] G. D. Finlayson and E. Trezzi, "Shades of gray and colour constancy," in *Proc. Color Imag. Conf.*, Jan. 2004, pp. 37–41.

[16] B. Funt and W. Xiong, "Estimating illumination chromaticity via support vector regression," in *Proc. Color Imag. Conf.*, Nov. 2004, pp. 47–52.

[17] G. D. Finlayson, S. D. Hordley, and I. Tastl, "Gamut constrained illuminant estimation," *Int. J. Comput. Vis.*, vol. 67, no. 1, pp. 93–109, Apr. 2006.

[18] S. D. Hordley, "Scene illuminant estimation: Past, present, and future," *Color Res. Appl.*, vol. 31, no. 4, pp. 303–314, Jul. 2006.

[19] J. van de Weijer, T. Gevers, and A. Gijsenij, "Edge-based color constancy," *IEEE Trans. Image Process.*, vol. 16, no. 9, pp. 2207–2214, Aug. 2007.

[20] P. V. Gehler, C. Rother, A. Blake, T. Minka, and T. Sharp, "Bayesian color constancy revisited," in *Proc. IEEE Conf. Comput. Vis. Pattern Recognit. (CVPR)*, Aug. 2008, pp. 1–8.

[21] A. Gijsenij, T. Gevers, and J. van de Weijer, "Generalized gamut mapping using image derivative structures for color constancy," *Int. J. Comput. Vis.*, vol. 86, no. 2, pp. 127–139, Jan. 2010.

[22] A. Chakrabarti, K. Hirakawa, and T. Zickler, "Color constancy with spatio-spectral statistics," *IEEE Trans. Pattern Anal. Mach. Intell.*, vol. 34, no. 8, pp. 1509–1519, Aug. 2012.

[23] G. D. Finlayson, "Corrected-moment illuminant estimation," in *Proc. IEEE Int. Conf. Comput. Vis. (ICCV)*, Dec. 2013, pp. 1904–1911.

[24] D. Cheng, D. K. Prasad, and M. S. Brown, "Illuminant estimation for color constancy: Why spatial-domain methods work and the role of the color distribution," *J. Opt. Soc. Amer. A, Opt. Image Sci.*, vol. 31, no. 5, pp. 1049–1058, May 2014.

[25] K.-F. Yang, S.-B. Gao, and Y.-J. Li, "Efficient illuminant estimation for color constancy using grey pixels," in *Proc. IEEE Conf. Comput. Vis. Pattern Recognit. (CVPR)*, Jun. 2015, pp. 2254–2263.

[26] S.-B. Gao, W. Han, K.-F. Yang, C.-Y. Li, and Y.-J. Li, "Efficient color constancy with local surface reflectance statistics," in *Proc. Eur. Conf. Comput. Vis. (ECCV)*, Sep. 2015, pp. 158–173.

[27] S. B. Gao, K. F. Yang, C. Y. Li, and Y. J. Li, "Color constancy using double-opponency," *IEEE Trans. Pattern Anal. Mach. Intell.*, vol. 37, no. 10, pp. 1973–1985, Oct. 2015.

[28] B. Li, W. Xiong, W. Hu, B. Funt, and J. Xing, "Multi-cue illumination estimation via a tree-structured group joint sparse representation," *Int. J. Comput. Vis.*, vol. 117, no. 1, pp. 21–47, Mar. 2016.

[29] Y. Hu, B. Wang, and S. Lin, "FC4: Fully convolutional color constancy with confidence-weighted pooling," in *Proc. IEEE Conf. Comput. Vis. Pattern Recognit. (CVPR)*, Nov. 2017, pp. 330–339.

[30] M. Afifi, A. Punnappurath, G. D. Finlayson, and M. S. Brown, "As-projective-as-possible bias correction for illumination estimation algorithms," *J. Opt. Soc. Amer. A, Opt. Image Sci.*, vol. 36, no. 1, pp. 71–78, Jan. 2019.

[31] Y. Qian, S. Pertuz, J. Nikkanen, J.-K. Kämäräinen, and J. Matas, "Revisiting gray pixel for statistical illumination estimation," in *Proc. 14th Int. Joint Conf. Comput. Vis., Imag. Comput. Graph. Theory Appl.*, 2019, pp. 36–46.

[32] S. Bianco and C. Cusano, "Quasi-unsupervised color constancy," in *Proc. IEEE/CVF Conf. Comput. Vis. Pattern Recognit. (CVPR)*, Jun. 2019, pp. 12212–12221.

[33] M. Afifi, B. Price, S. Cohen, and M. S. Brown, "When color constancy goes wrong: Correcting improperly white-balanced images," in *Proc. IEEE/CVF Conf. Comput. Vis. Pattern Recognit. (CVPR)*, Jun. 2019, pp. 1535–1544.

[34] M. Afifi and M. S. Brown, "Deep white-balance editing," in *Proc. IEEE/CVF Conf. Comput. Vis. Pattern Recognit.*, Jun. 2020, pp. 1397–1406.

[35] S. Bianco, G. Ciocca, C. Cusano, and R. Schettini, "Automatic color constancy algorithm selection and combination," *Pattern Recognit.*, vol. 43, no. 3, pp. 695–705, Mar. 2010.

[36] A. Gijsenij and T. Gevers, "Color constancy using natural image statistics and scene semantics," *IEEE Trans. Pattern Anal. Mach. Intell.*, vol. 33, no. 4, pp. 687–698, Apr. 2011.

[37] H. R. V. Joze and M. Drew, "Exemplar-based colour constancy," in *Proc. Brit. Mach. Vis. Conf.*, 2012, pp. 1–12.

[38] T. Akazawa, Y. Kinoshita, and H. Kiya, "Multi-color balancing for correctly adjusting the intensity of target colors," in *Proc. IEEE 3rd Global Conf. Life Sci. Technol. (LifeTech)*, Mar. 2021, pp. 8–12.

[39] T. Akazawa, Y. Kinoshita, S. Shiota, and H. Kiya, "Three-color balancing for color constancy correction," *J. Imag.*, vol. 7, no. 10, p. 207, Oct. 2021.

[40] T. Akazawa, Y. Kinoshita, and H. Kiya, "Spatially varying white balancing for mixed and non-uniform illuminants," in *Proc. APSIPA Annu. Summit Conf.*, Dec. 2021, pp. 1571–1575.

[41] M. Ebner, "Color constancy using local color shifts," in *Proc. Eur. Conf. Comput. Vis. (ECCV)*, May 2004, pp. 276–287.

[42] A. Gijsenij, R. Lu, and T. Gevers, "Color constancy for multiple light sources," *IEEE Trans. Image Process.*, vol. 21, no. 2, pp. 697–707, Feb. 2012.

[43] S. Beigpour, C. Riess, J. van de Weijer, and E. Angelopoulou, "Multi-illuminant estimation with conditional random fields," *IEEE Trans. Image Process.*, vol. 23, no. 1, pp. 83–96, Jan. 2014.

[44] D. Cheng, A. Kamel, B. Price, S. Cohen, and M. S. Brown, "Two illuminant estimation and user correction preference," in *Proc. IEEE Conf. Comput. Vis. Pattern Recognit. (CVPR)*, Jun. 2016, pp. 469–477.

[45] M. A. Hussain and A. S. Akbari, "Color constancy algorithm for mixed-illuminant scene images," *IEEE Access*, vol. 6, pp. 8964–8976, 2018.

[46] M. Afifi, M. A. Brubaker, and M. S. Brown, "Auto white-balance correction for mixed-illuminant scenes," in *Proc. IEEE/CVF Winter Conf. Appl. Comput. Vis. (WACV)*, Jan. 2022, pp. 1210–1219.
[47] K. Barnard, G. D. Finlayson, and B. Funt, "Colour constancy for scenes with varying illumination," in *Proc. Eur. Conf. Comput. Vis. (ECCV)*, Apr. 1996, pp. 1–15.
[48] X.-S. Zhang, S.-B. Gao, R.-X. Li, X.-Y. Du, C.-Y. Li, and Y.-J. Li, "A retinal mechanism inspired color constancy model," *IEEE Trans. Image Process.*, vol. 25, no. 3, pp. 1219–1232, Jan. 2016.
[49] S.-B. Gao, Y.-Z. Ren, M. Zhang, and Y.-J. Li, "Combining bottom-up and top-down visual mechanisms for color constancy under varying illumination," *IEEE Trans. Image Process.*, vol. 28, no. 9, pp. 4387–4400, Mar. 2019.
[50] W. Xiong and B. Funt, "Color constancy for multiple-illuminant scenes using Retinex and SVR," in *Proc. Color Imag. Conf.*, Jan. 2006, pp. 304–308.
[51] S. Bianco, C. Cusano, and R. Schettini, "Single and multiple illuminant estimation using convolutional neural networks," *IEEE Trans. Image Process.*, vol. 26, no. 9, pp. 4347–4362, Sep. 2017.
[52] O. Sidorov, "Conditional GANs for multi-illuminant color constancy: Revolution or yet another approach?" in *Proc. IEEE/CVF Conf. Comput. Vis. Pattern Recognit. Workshops (CVPRW)*, Jun. 2019, pp. 1–11.
[53] G. Finlayson and R. Zakizadeh, "Reproduction angular error: An improved performance metric for illuminant estimation," in *Proc. Brit. Mach. Vis. Conf.*, Sep. 2014, p. 1.
[54] J. H. Lambert, *Photometria, sive de Mensura et Gradibus Luminis, Colorum et Umbrae*. Augsburg, Germany: Klett, 1760.
[55] Y. Qian, J.-K. Kamarainen, J. Nikkanen, and J. Matas, "On finding gray pixels," in *Proc. IEEE Conf. Comput. Vis. Pattern Recognit.*, Jun. 2019, pp. 8062–8070.
[56] J. T. Barron and Y.-T. Tsai, "Fast Fourier color constancy," in *Proc. IEEE Conf. Comput. Vis. Pattern Recognit. (CVPR)*, Jul. 2017, pp. 886–894.
[57] D. Hernandez-Juarez, S. Parisot, B. Busam, A. Leonardis, G. Slabaugh, and S. McDonagh, "A multi-hypothesis approach to color constancy," in *Proc. IEEE/CVF Conf. Comput. Vis. Pattern Recognit. (CVPR)*, Jun. 2020, pp. 2270–2280.
[58] *Chromatic Adaptation*. Accessed: Mar. 11, 2022. [Online]. Available: http://www.brucelindbloom.com/index.html?Eqn_ChromAdapt.html
[59] J. von Kries, "Beitrag zur physiologie der gesichtsempfindung," *Arch. Anatomy Physiol.*, vol. 2, pp. 503–524, 1878. [Online]. Available: https://www.biodiversitylibrary.org/item/109724
[60] H. Y. Chong, S. J. Gortler, and T. Zickler, "The von kries hypothesis and a basis for color constancy," in *Proc. IEEE 11th Int. Conf. Comput. Vis.*, Oct. 2007, pp. 1–8.
[61] K. M. Lam, "Metamerism colour constancy," Ph.D. thesis, Postgraduate School Colour Chem. Colour Technol., Univ. Bradford, Bradford, U.K., 1985.
[62] G. D. Finlayson and S. Süsstrunk, "Spectral sharpening and the Bradford transform," in *Proc. Color Imag. Symp. (CIS)*, Jan. 2000, pp. 236–243.
[63] E. Hsu, T. Mertens, S. Paris, S. Avidan, and F. Durand, "Light mixture estimation for spatially varying white balance," *ACM Trans. Graph.*, vol. 27, no. 3, pp. 1–7, Aug. 2008.
[64] S. Yan, F. Peng, H. Tan, S. Lai, and M. Zhang, "Multiple illumination estimation with end-to-end network," in *Proc. IEEE 3rd Int. Conf. Image, Vis. Comput. (ICIVC)*, Jun. 2018, pp. 642–647.
[65] D. Kim, J. Kim, S. Nam, D. Lee, Y. Lee, N. Kang, H.-E. Lee, B. Yoo, J.-J. Han, and S. J. Kim, "Large scale multi-illuminant (LSMI) dataset for developing white balance algorithm under mixed illumination," in *Proc. IEEE/CVF Int. Conf. Comput. Vis. (ICCV)*, Oct. 2021, pp. 2390–2399.

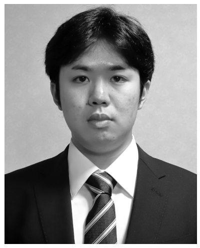

TERUAKI AKAZAWA (Student Member, IEEE) received the B.Eng. degree from Tokyo Metropolitan University, Japan, in 2021, where he is currently pursuing the master's degree. His research interest includes image processing.

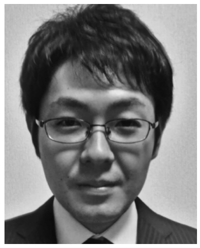

YUMA KINOSHITA (Member, IEEE) received the B.Eng., M.Eng., and Ph.D. degrees from Tokyo Metropolitan University, Japan, in 2016, 2018, and 2020, respectively. In April 2020, he started to work with Tokyo Metropolitan University, as a Project Assistant Professor. He moved to Tokai University, Japan, as an Associate Professor/Lecturer, in April 2022. His research interests include signal processing, image processing, and machine learning. He is a member of APSIPA, IEICE, and ASJ. He received the IEEE ISPACS Best Paper Award in 2016, the IEEE Signal Processing Society Japan Student Conference Paper Award in 2018, the IEEE Signal Processing Society Tokyo Joint Chapter Student Award in 2018, the IEEE GCCE Excellent Paper Award (Gold Prize) in 2019, and the IWAIT Best Paper Award in 2020. He was a Registration Chair of DCASE2020 Workshop.

SAYAKA SHIOTA (Member, IEEE) received the B.E., M.E., and Ph.D. degrees in intelligence and computer science, engineering, and engineering simulation from the Nagoya Institute of Technology, Nagoya, Japan, in 2007, 2009, and 2012, respectively. From February 2013 to March 2014, she worked as a Project Assistant Professor at the Institute of Statistical Mathematics. In April 2014, she joined Tokyo Metropolitan University, as an Assistant Professor. She is a member of ASJ, IPSJ, IEICE, APSIPA, and ISCA.

HITOSHI KIYA (Life Fellow, IEEE) received the B.E. and M.E. degrees from the Nagaoka University of Technology, in 1980 and 1982, respectively, and the Dr.Eng. degree from Tokyo Metropolitan University, in 1987. In 1982, he joined Tokyo Metropolitan University, where he became a Full Professor, in 2000. From 1995 to 1996, he attended the University of Sydney, Australia, as a Visiting Fellow. He is a fellow of IEICE, AAIA, and ITE. He has received numerous awards, including 12 best paper awards. He has organized a lot of international conferences in roles, such as the TPC Chair of the IEEE ICASSP 2012 and as the General Co-Chair of the IEEE ISCAS 2019. He served as the President for the APSIPA, from 2019 to 2020, and as the Regional Director-at-Large for Region 10 of the IEEE Signal Processing Society, from 2016 to 2017.